Intense Pulsed Neutron Source Target Integrity

J.R. Ball, H.U. Ahmed, B.A. Loomis
Argonne National Laboratory,
9700 South Cass Avenue, Argonne, Illinois 60439, U.S.A.

SUMMARY

The need for new high-flux neutron research facilities has been extensively discussed in the international scientific community. These discussions have become increasingly focused on pulsed neutron sources. Pulsed neutron sources avoid some of the problems associated with reactor-based sources, e.g., heat removal, U^{235} and Pu^{239} inventory, and fuel cost, by producing intense bursts of neutrons for only a small portion of the time. At Argonne National Laboratory, the concept of a pulsed spallation neutron source has been theoretically and experimentally investigated in the form proposed by Carpenter [1]. In this type of source, a pulsed beam of protons (30 Hz) is accelerated in a synchrotron to medium energy ($\sim$1 GeV) and and then projected onto a heavy metal target, e.g., uranium, tantalum, or tungsten, resulting in the emission of large quantities of neutrons by the excited target nuclei. Since the energy deposited by the energetic protons and liberated by the nuclear reactions in the target material is non-uniform, significant levels of thermally induced stress are developed in the target and target-cladding material. In this paper we present theoretical analyses and experimental results pertaining to the thermal and mechanical response of Zircaloy-2- and zirconium-clad uranium targets in an Intense Pulsed Neutron Source (IPNS) situation.

The stress analysis of the target was performed by using simplified finite-element elastic methods. The analysis included the effects of cyclic temperature loadings generated by the start-up and shutdown of the proton source. Because of these loadings, the stress analysis had to include the effects of creep, thermal ratcheting, irradiation-induced physical and mechanical property changes, and fatigue behavior of the target.

To verify the results of the theoretical stress analysis, experiments were carried out on prototype target discs. These prototype experiments were performed under cyclic thermal loadings similar to expected target operating conditions. Results are presented for both ZING-P' and IPNS-I target conditions. The material presented in this paper is a unique set of analytical thermal and stress analyses and experimental verification for a biaxial geometry.

*Based on work performed under the auspices of the Department of Energy.

I. Introduction

The Intense Pulsed Neutron Source (IPNS) program at Argonne National Laboratory (ANL) is a multiphase effort directed toward the construction, operation and utilization of a high-intensity pulsed spallation neutron source for materials research using fast and thermal neutrons. The design of the IPNS-I target is the result of a two-year effort involving theoretical analyses, prototypic target operation, and experimental verification of the thermal and mechanical responses of Zircaloy-2- clad (IPNS-1 experiment) and zirconium-clad (ZING-P' experiment) uranium targets in a pulsed-neutron source environment.

Several factors present in the operation of the uranium target act to degrade the target integrity, possibly to the point of failure. Failure of the target is defined as the release of radioactive spallation and fission products into the cooling stream by rupture of the uranium cladding. The non-uniform temperature distribution in the target gives rise to thermal stresses in the uranium and cladding material. Because of the inherent on-and-off nature of synchrotron operation, (10-15 interruptions per day), these thermal stresses increase during target heating and diminish as the target cools during the off cycle. These cyclic stresses can produce fatigue in the target materials. In addition, the clad target is in a state of high residual stress as a result of the Hot Isostatic Bonding (HIP) process used for cladding uranium. Finally, the uranium is subject to several swelling mechanisms over the life of the target, which create swelling-induced stresses in the uranium and cladding. The ultimate failure of the target is a synergistic effect of all these stresses. The goal of the analytical and design program was to arrive at a target design for which the overall mechanical analysis would show that a minimum target lifetime of one year could be expected for a 500 MeV proton beam of 22 μamps.

2. Geometry

2.1 ZING-P'

A report containing a detailed description of the ZING-P' target geometry is currently in preparation at ANL. A summary of the design description has been reported by Wehrle et al.[2].

2.2 IPNS-I

An isometric drawing of the IPNS-I target assembly is shown in Fig. 1a. The target consists of eight Zircaloy-2-clad U discs, each 4 in. in diameter and 1 in. thick. The discs are positioned on edge and separated by disc containers to support them and provide coolant-flow passages between the faces of the discs. The stack of discs is loaded into a housing which acts as a secondary containment and pressure boundary for the target cooling water. The stack is spring loaded within the housing to allow for thermal expansion and contraction during the start-up and shutdown of the accelerator and to allow for the irradiation-induced dimensional changes of the U over the lifetime of the target. The target assembly is approximately 5-1/8 in. in diameter and 12-1/2 in. long overall.

Cooling water (demineralized light water) enters through the rear housing cover and is diverted to the inlet plenum along the top of the housing. The water passes through the flow channels of the disc containers, which are in direct contact with the cladding material on the faces of each disc. The coolant is collected in the outlet plenum and is carried out of the target to a heat-exchanger system..

The proton beam is projected onto the front face of the target. As the protons pass through the U discs, the proton interactions with the U nuclei result in production ~20 neutrons per incident proton. The proton beam is absorbed in the 8-in. length of U. The nuclear reactions are also the source of internal heating within the discs.

Figure 1b shows a single target disc and disc container. The disc is clad with 0.02 in. of Zircaloy-2 on the faces and 0.06 in. on the cylindrical surface. The disc container provides five channels for flow of coolant water across each target face. The width and depth of the channels are shown in Fig. 1b. Each of the discs in positions 1, 3, 5, and 7 contain a well for insertion of a thermocouple to allow monitoring of the disc centerline temperature during operation.

Experimental data from the operation of the ZING-P' target confirmed that the axial location of highest energy deposition is 2 in. from the front face for 0.5-GeV protons. Therefore, the target disc in position 2 was chosen for detailed analysis.

3.0 Dimensional Changes

The processes which can result in dimensional changes of U in a pulsed neutron source application are formation of solid and gaseous spallation products [3,4], formation of solid and gaseous fission products [5], formation of spallation- and fission-gas bubbles [4,6], cavitational swelling [7], irradiation-induced growth [8], thermal cycling-induced growth [9], and thermal expansion. The dimensional changes caused by these processes can be minimized by adding alloying elements, e.g., C, Si, Fe, and Al, to the U; operating the U target below a well-defined temperature; and manipulating the U production procedure to obtain certain microstructural characteristics, e.g., moderate grain size and random grain orientation. Two additional factors must be considered in the alloying of U for dimensional stability: spallation neutron production in a material is proportional to the atomic weight [10], and fast neutron production in U is diminished by the addition of elements with a low probability of fissioning by energetic neutrons.

Guidance in the selection of the alloying elements to be added to U and the operating temperature of the target were obtained from the extensive investigations reported in the literature on the dimensional stability of U during irradiation in nuclear reactors. We have selected a U alloy containing a nominal 450 ppm C, 250 ppm Fe, and 350 ppm Si for production and evaluation as a target material for the intense pulsed neutron source.

The continuous pulsing of the proton beam at 30 Hz induces temperature cycles of < 1°F in the U for target temperatures less than 660°F. However, if the proton source is subject to several start-up/shutdown cycles, then the dimensional instability of U is greatly exacerbated by thermal cycling between 120°F and the operating temperature, especially above 660°F [9]. The dimensional instability or "growth" of U on thermal cycling is due to the anisotropic crystal structure of U [9]. Previous experience with synchrotron operations suggests that 10-15 interruptions per day can be expected; each results in cooling of the target to approximately ambient temperature (120°F). Since the highest "growth" rate occurs in U with highly preferred orientation of the individual grains coupled with a small grain size, the target production procedure should incorporate steps to obtain a nearly-random grain orientation and a grain diameter $\gtrsim$ 0.004 in. This can be accomplished by heating and cooling of the U through the alpha-beta phase transformation at 1221°F [9]. The grain size of the U should not be too large since anisotropic growth of individual grains at the U surface results in surface roughening [9]. The total $\Delta L/L$ of the U in one year due to the combined processes of the irradiation effects (0.009) and thermal expansion (0.005) is expected to be 0.014 if the target is operated at a maximum U temperature of 660°F. This total $\Delta L/L$ per year is regarded as a maximum value since consideration has not been given to the possible restraining influence of a Zircaloy-2 cladding that will be required. It is believed that this dimensional change will be easily accommodated by the design of the target housing and will not contribute significantly to degradation of the target discs in one year of operation.

4.0 Thermal Analysis

The analysis of the thermal behavior of the ZING-P' and IPNS-I targets under proton irradiation is a two-fold problem. As a first step, it is necessary to evaluate the heat generation rates in the U target material due to the proton bombardment. Secondly, given a knowledge of the internal heat generation rates and the associated boundary conditions, it is then possible to compute the target temperature distributions.

Temperatures were computed in the Zr-clad ZING-P' and Zircaloy-2-clad IPNS-I targets by the ANSYS computer code using heat generation rates furnished by nucleon-transport calculations [11]. It is assummed that no heat generation occurs in the cladding, and that cooling at the boundary occurs by convection via a forced circulating water flow.

For a cylindrical geometry with axial symmetry, the time-dependent thermal behavior in the presence of internal heat generation is described by

$$\frac{1}{\alpha}\frac{\partial T}{\partial t} = \frac{\partial^2 T}{\partial r^2} + \frac{1}{r}\frac{\partial T}{\partial r} + \frac{\partial^2 T}{\partial Z^2} + \frac{1}{K} q''(r,Z) \qquad (1)$$

where $\alpha = K/\rho C_p$, K is the U thermal conductivity, ρ is the U density, C_p is the U specific heat at constant pressure, and q" is the heat generation rate. Temperature-dependent properties are used for α, K, and C_p. For this problem, the steady-state solution is conservative with respect to the transient solution, since the maximum temperatures are reached in the steady state. The heat transfer coefficients and material properties used in the calculations are given in Ref. [12].

A study was conducted to determine the pressure drops, velocity, and pressure profiles of the cooling water in the target assembly (see Fig. 2). The Hydraulic Network Analysis (HYNAL) computer program developed by Logicomp Corporation was employed for these computations. This program employs the Hardy-Cross method which is based on relaxation or controlled trial and error. The network to be analyzed is limited to a maximum of 500 pipes, 200 loops, and 300 junctions.

The HYNAL program uses the Hazen-Williams formula to calculate the pressure drop due to friction. This formula is given by

$$\Delta H = \frac{10.43L}{C^{1.85}\,D^{4.87}}\,Q^{1.85} \qquad (2)$$

where

ΔH = head loss, ft. of water,
L = length of pipe, ft.,
D = inside diameter of pipe, inches,
Q = flow, gpm,
and C = constant which depends on surface roughness.

For our case, the values of C have to be estimated for a trial run and then refined for more accurate results. This procedure is discussed in Ref. [12].

The power distribution calculated by the Nuclear Transport Codes (HECTC/VIM) for IPNS-I target is given in Table 1. This calculated distribution was adjusted from measured values obtained from operation of the ZING-P[1] prototype target. The finite element computer code ANSYS, was then used to calculate the resulting temperature distribution within the IPNS-I target using an axisymmetric element (see Ref. 12).

Because of the dependence on an axisymmetric finite-element model, it is not possible to treat the slotted geometry exactly. Instead, the heat transfer characteristics of the target disc are cylindrically averaged to derive effective convective coefficients within concentric zones.

The simplest approach employed in the thermal analysis is called the 1-convective zone approach. In the 1-zone method, an effective value of the convective coefficient h is computed for the entire disc face (assumed to be 1 convective zone), based on an averaging of the individual channel heat transfer coefficients over the face of the disc. Since the convective coefficient h is a function of the coolant film temperature, which is not precisely known in advance, an iterative procedure is required to arrive at a consistent solution for h.

The 1-zone approach is inherently conservative. Since the heat flux is greatest toward the center of the disc where the temperature is highest, the actual convective coefficient at the center is larger than the assumed average value. Accordingly, the actual center temperatures are lower than the calculated temperatures using the 1-zone approach. Conversely, near the edge of the disc, the actual convective coefficient is lower than the assumed average value; however, since the heat generation rate near the disc edge is very low, the actual temperatures near the edge remain low compared to the center temperatures.

The 1-convective zone scheme suffers from the added drawback that distinctions in thermal performance between target geometries differing, for example, in channel arrangement are obscured by the averaging procedure. In the present study where it is desired to gauge the effectiveness of a 5-channel geometry with channels concentrating the cooling at the center against a 7-channel geometry resulting in relatively uniform cooling, such distinctions are important.

In an attempt to alleviate some of the shortcomings of the 1-zone approach while maintaining the simplicity of the axisymmetric model, an additional scheme--the 2-convective zone approach-- has been employed. In the 2-zone approach, the disc is divided into two concentric zones: an inner circle of 1-in radius, and the remaining outer ring. An effective convective coefficient is separately computed for each zone by averaging the individual channel heat transfer coefficients within the respective zone. A trail and error approach is required to arrive at convective coefficients consistent with the average coolant film temperature in each zone. Although the 2-zone calculations are expected to provide more realistic temperatures, 1-zone calculations are also made to provide more conservative thermal inputs for the target stress analysis and fatigue life evaluation.

4.1 IPNS-I Tempertures

The 1-zone approach is overly conservative where a large temperature variation occurs between the disc center and edge. Accordingly, only 2-zone results are furnished for the reduced-flow cases. The blocked-channel case is effectively a 3-zone calculation, since the convective coefficient is set to zero in a 3/4-in. diameter circle centered on the disc face. Contour plots of the temperature distributions for various flow conditions are shown in Fig. 3. In all of the full-flow cases, the results indicate that the water flow is well below the nucleate-boiling regime (T_{sat} = 260°F).

5. Heat Treatment Effects

Evaluation of the effect of the HIP bonding process on the residual stress is predominantly determined by accurate treatment of the coefficient of thermal expansion. Temperature polynomials for the mean coefficient of thermal expansion for Zr, Zircaloy-2, and U are given below

Zr $\qquad \bar{\alpha} = 3.11 \times 10^{-6} + .0017 \times 10^{-6} T$ IN/IN - °F, (T_{REF} = 68°F)

for T = 932°F, $\bar{\alpha} = 4.77 \times 10^{-6}$ IN/IN - °F; (3)

Zircaloy-2 $\qquad \bar{\alpha} = 3.11 \times 10^{-6} + .00095 \times 10^{-6}$ IN/IN - °F, (T_{REF} = 68°F)

for T = 932°F, $\bar{\alpha} = 4.00 \times 10^{-6}$ IN/IN - °F; (4)

U $\qquad \bar{\alpha} = 8.17 \times 10^{-6} + .0017 \times 10^{-6}$ IN/IN - °F, (T_{REF} = 68°F)

for T = 932°F, $\bar{a} = 9.75 \times 10^{-6}$ IN/IN - °F . (5)

Since these mean coefficients of thermal expansion are measured values with respect to a reference temperature, some adjustment in these values is required when the reference temperature is different than the one used in evaluating IPNS-I heat treatment effects. It should be noted, that for both IPNS-I and ZING-P' experiments, the reference zero-stress temperature is 932°F rather than room temperature. The residual stress state was achieved by specifying a reference temperature of 932°F corresponding to a zero-stress level, and then cooling to a uniform temperature of 70°F throughout the target. Since the zero-stress temperature (reference) is different from the temperature upon which the coefficient of thermal expansion α is based, an effective coefficient of thermal expansion, α_{eff}, is obtained from the equation

$$\alpha_{eff}(T_1) = \alpha(T_1) + \frac{\alpha(T_1) - \alpha(T_{REF})}{T - T} (T_{REF} - T_0) \qquad (6)$$

6. Fatigue Analysis

Evaluation of fatigue damage for the IPNS-I target, corresponding to power cycles at 22 microamp of proton beam current was made by use of Miner's damage rule and stresses in Fig. 4 and 5 in conjunction with cycles-to-failure charts developed by W. O'Donnel, et al, in Ref. [13].

Miner's damage rule is given by [14]

$$\sum_{j=1}^{P} \left(\frac{n}{N_d}\right)_j + \sum_{k=1}^{q} \left(\frac{t}{T_d}\right)_k < D \qquad (7)$$

Where D = total creep-fatigue damage;

n = number of applied cycles of loading conditions, j;

N_d = number of design allowable cycles of loading condition, j, from one of the fatigue design curves in Ref. (13) corresponding to the maximum metal temperature during the cycle;

t = duration of the load condition, K; and

T_d = allowable time at a given stress intensity (for elastic analysis) or at a given effective stress (for inelastic analysis) from load, K.

T_d values are obtained by entering the stress-to-rupture curve at a stress value equal to the calculated stress from load K. When creep effects are negligible (such as is the case for IPNS-I target) T_d is much larger than t so that the second term of Eq. (7) is neglible.

The design fatigue curves of Ref. [13] include the effect of high mean stress in Zircaloy cladding and are applicable to the results obtained from elastic analysis. The fatigue design curves in Fig. 6 are based on a built-in safety factor of 2 on stress amplitude or a factor of 20 on cycles, whichever is more conservative at each point. These safety factors are believed to be sufficient to cover the effect of size, environment, surface finish and scatter of data.

In Fig. 6, $S_{alt} = 1/2\ \varepsilon_t E$ is the completely reversed induced-stress amplitude. However Ref. [12] suggests for the determination of S_{alt}, the relation

S_{alt} = 1/2 the maximum of $|\sigma_1 - \sigma_2|$, $|\sigma_2 - \sigma_3|$. $|\sigma_1 - \sigma_3|$, where σ_1, σ_2 and σ_3 are the three principal stresses such that $\sigma_1 < \sigma_2 < \sigma_3$. The finite element analysis of the IPNS-I target for the principal stresses has shown that σ_1 = 42,644 psi, σ_2 = 42,409 psi and σ_3 = 427 psi. Therefore, S_{alt} is 21,108 psi. From Fig. 6 the allowable number of stress cycles is 3000 for irradiated Zircaloy and 6000 for unirradiated material. For the first year of operation, IPNS-I target material may be considered to correspond to unirradiated material (Fig. 6) and thereafter it would correspond to irradiated material.

7. Thermal Cycling Test

The design analysis has shown that the primary failure mode for a Zircaloy-clad U disc in the target of the pulsed neutron source considered in this paper is expected to be crack form ation and propagation in the Zircaloy-2 cladding. The cracks are considered to result from the repetitive (10-15 cycles per day) production of stresses, i.e., fatigue failure, in the Zircaloy -2 cladding as the U temperature varies between ambient temperature (120°F) and 660°F.

We have experimentally investigated the response of an as-produced Zircaloy-clad U disc to thermal cycling at temperatures between 280 and 660°F. The dimensional change of the disc and the integrity of the Zircaloy-U bond were determined at 1000-cycle intervals by ultrasonic inspection and dimensional measurements. These results showed no measurable change in either the dimensions of the disc or the integrity of the Zircaloy-U bond after 6000 cycles. However, on removal of the disc for examination after 7000 cycles, a crack was visually observed in the Zircaloy cladding on a face of the disc. The crack (0.16-in. length) appeared to have propagated in a ductile manner ad was located at 0.4-in radial distance from the axis of the disc. Even though the Zircaloy was machined to a 1-microinch surface finish, there was some evidence to indicate that the crack was initiated and propagated along a machining-tool groove.

8. Conclusions

Based on the stress analyses and the thermal-cycling results, it is believed that the Zircaloy-2-clad U target can be operated for at least one year without failure of the cladding under the expected conditions, namely, 22μa (30 Hz) of 500 MeV-proton beam current.

References

[1] Carpenter, J., et al, Nuclear Instru. and Methods 145, 91 (1977.

[2] Wehrle, R. B., et al, "The Uranium 238 Target of the Zing-P' Pulsed Spallation Neutron Source," Argonne National Laboratory (in preparation).

[3] Barbier, M. Induced Radioactivity, North-Holland, London (1969) p. 95.

[4] Coulter, C. A., Parkin, D. M., and Green, W. V., J. Nucl. Mater., 67, 140 (1977).

[5] Brinkman, J. A., Nuclear Metallurgy, Vol. VI, (Symposium on Effects of Irradiation on Fuel and Fuel Elements, Chicago, 1959, Met. Soc. AIME), pp. 1-11.

[6] Loomis, B. A., and Gerber, S. B., J. Nucl. Mater., 16, 49 (1965).

[7] McDonnell, W. R., Proc. 1973 Int. Conf. on Physical Metallurgy of Reactor Fuel Elements, Gloucestershire, England, ed. by J. E. Harris and E. C. Sykes, The Metals Society, pp. 266-274.

[8] Loomis, B. A. and Gerber, S.B., Phil. Mag. 18, 539 (1968).

[9] Foote, F. G., Progress in Nuclear Energy, Vol. 1, Series V (1956), p. 81.

[10] Carpenter, J. H., Nucl. Instrum. and Methods, 145, 91 (1977).

[11] Personal communication from H. Hubeny to J. Carpenter, Jan. 1981, Argonne National Laboratory.

[12] Carpenter, J., et al, "An Evaluation of Structural Integrity of IPNS-I and Zing-P' Targets, Argonne National Laboratory (in preparation).

[13] O'Donnel, W. J., and Langer, B. F., Nuclear Science and Engineering, 20,1 (1964).

[14] ASME Nuclear Vessel Code - Section III - Code Case 1592 (1979).

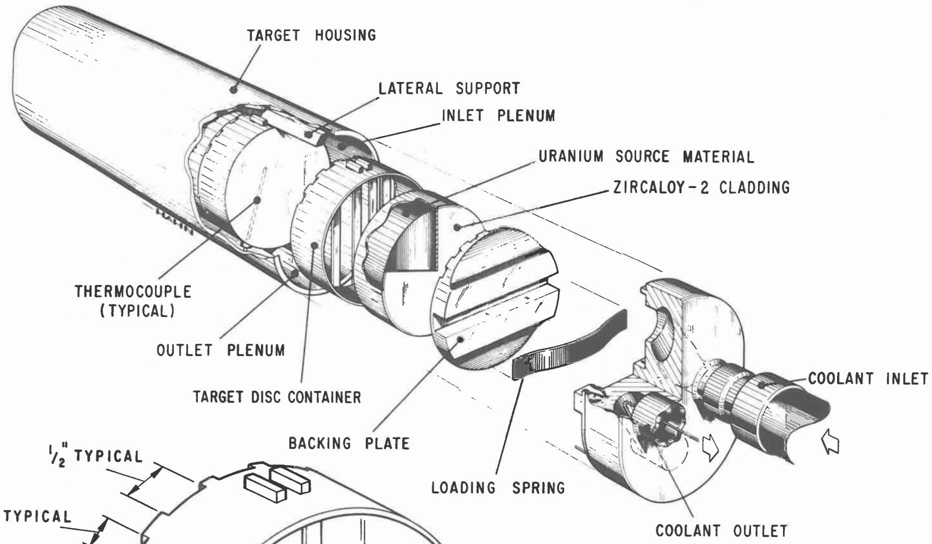

(a) IPNS-I Target

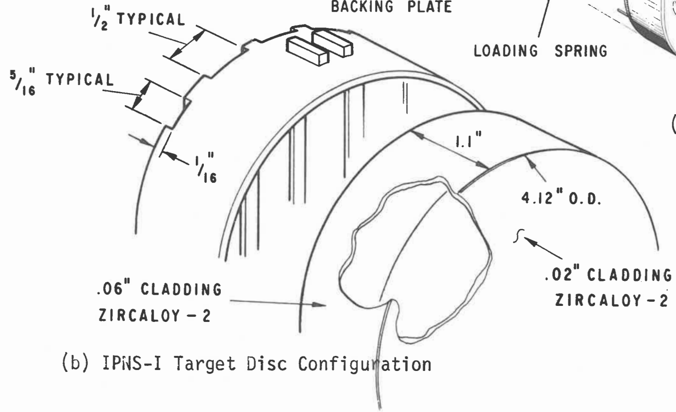

(b) IPNS-I Target Disc Configuration

Fig.1. IPNS-I Target and Disc Geometries

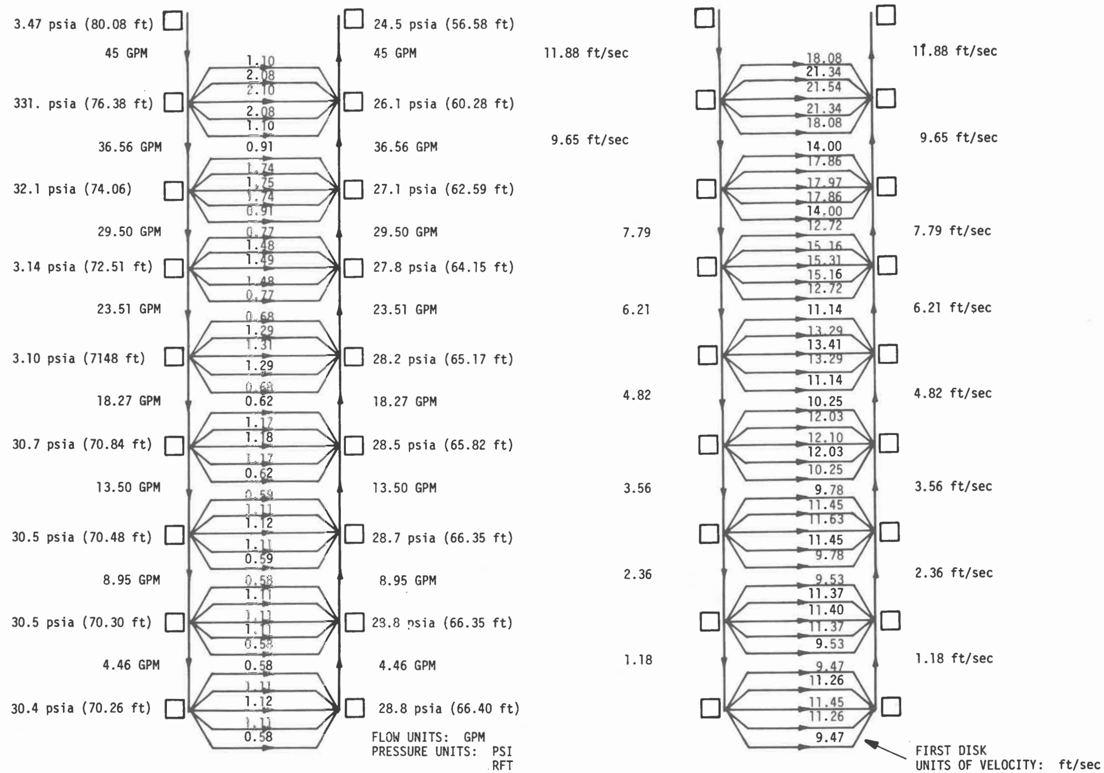

(a). **Flow and Pressure Profile.**

(b). **Velocity Distribution.**

Fig.2. Flow,Pressure, and Velocity Profiles in
IPNS-I Target Cooling System.

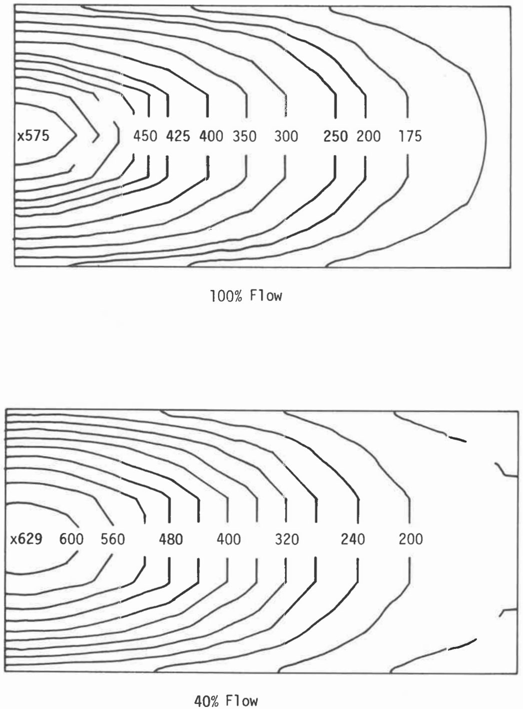

Fig.3. Temperature Distributions in IPNS-I Target Disc.

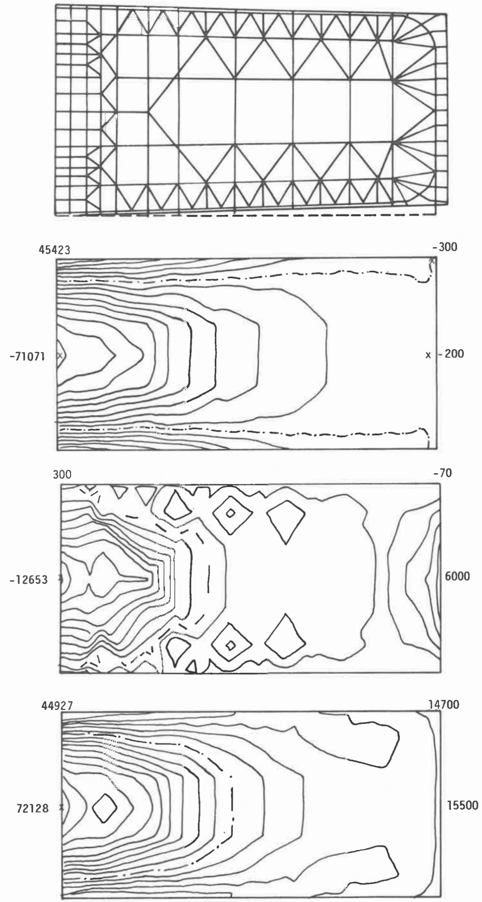

(a) IPNS-I Target-
Deflected Shape (solid line)
Due to Power Cycle (Dot line
indicates undeflected shapes)
(Uran. t=1 in. case).

(b) Radial stress (psi)
Distribution (stress difference
of 8000 psi).

(c) Axial stress (psi)
Distribution (stress difference
of 1500 psi).

(d) Hoop Stress (psi)
Distribution (stress difference
of 8000 psi).

Fig.4. IPNS-I Target Disc Stress Distribution-I

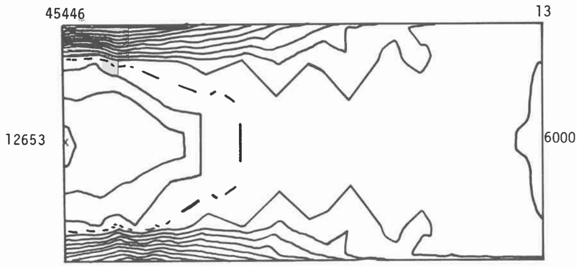

(e) Max Principle Stress (psi) (stress difference of 4000 psi).

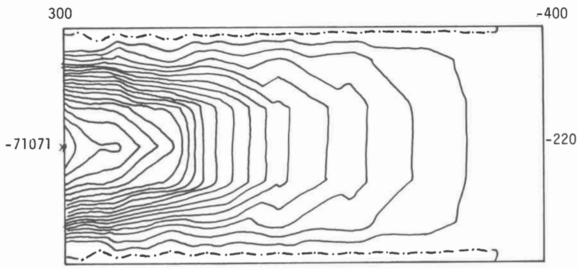

(f) Min. Principle Stress Distribution (stress difference of 4000 psi between contour lines).

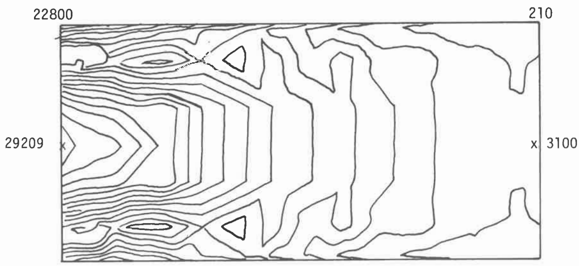

(g) Principle Shear Stress (psi) Distribution (stress difference of 2000 psi).

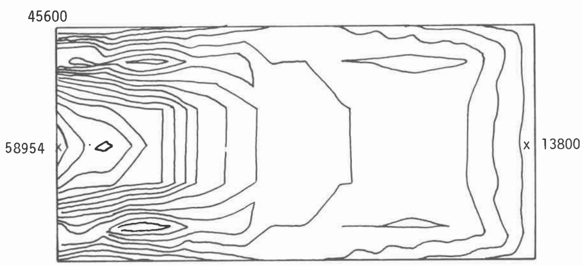

(h) IPNS-I Target Effective stress (psi) Distribution Due to Power Cycle (stress difference of 4000 psi between contour lines). (Uran. t-1" case).

Fig.5. IPNS-I Target Disc Stress Distribution-II

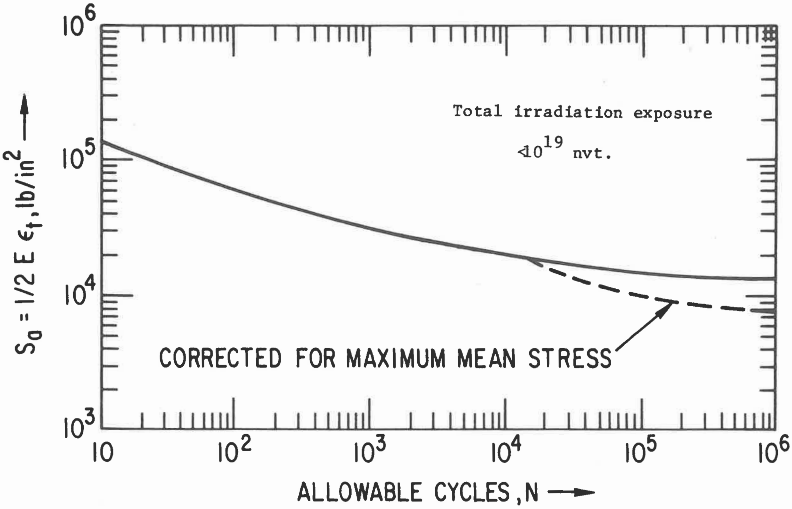

(a). Design Curve for Unirradiated Zircaloy-2, 3, or 4. Room Temperature to 600°F.

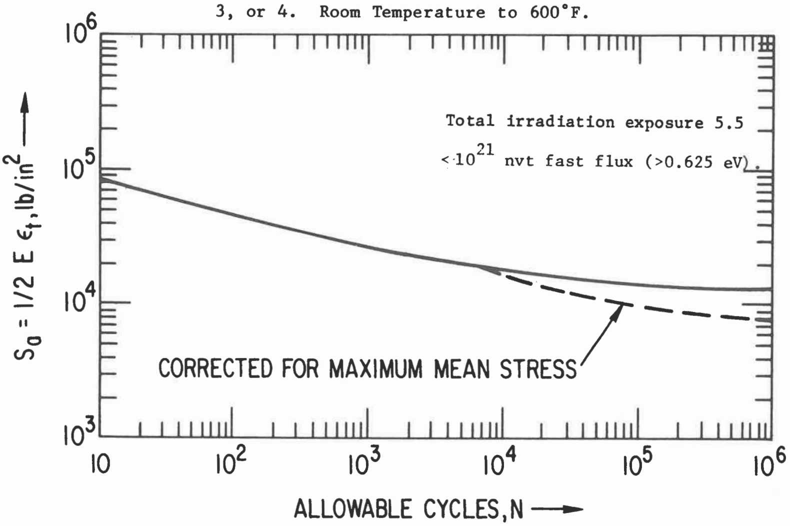

(b). Design Curve for Irradiated Zircaloy-2, 3, or 4. Room Temperature to 600°F.

Fig.6. Design Fatigue Curves for Zircaloy Cladding.

Table 1 HETC/VIM Thermal Energy Deposition for IPNS-I Target with Beryllium Reflector. 500 MeV, 1 μa beam, FWHM=4 cm, Parabolic Beam Profile

POWER DENSITY (WATT/CC)

Radial Region

Axial Region	0-1 cm	1-2 cm	2-3 cm	3-4 cm	4-5.3 cm
0-2 cm	2.663	1.913	0.895	0.206	0.072
2-4	2.468	1.836	0.881	0.228	0.100
4-6	2.121	1.634	0.783	0.250	0.105
6-8	1.766	1.348	0.698	0.232	0.103
8-10	1.444	1.113	0.613	0.244	0.093
10.12	1.202	0.983	0.556	0.236	0.084
12-14	1.063	0.874	0.547	0.250	0.084
14-16	0.050	0.047	0.039	0.038	0.031
16-18	0.023	0.025	0.025	0.027	0.026
18-20	0.021	0.019	0.020	0.014	0.013
20-22	0.012	0.014	0.012	0.012	0.010